Two-pulse echo experiments in the spectral diffusion regime

Mark A. Berg[a)]
Department of Chemistry and Biochemistry, University of South Carolina, Columbia, South Carolina 29208

K. D. Rector[b)] and M. D. Fayer
Department of Chemistry, Stanford University, Stanford, California 94305

(Received 13 March 2000; accepted 24 May 2000)

The two-pulse echo sequence is examined for the case in which the frequency modulation time τ_m of the transition is intermediate between the well known limiting cases of very fast modulation (motional narrowing) and very slow or static modulation (inhomogeneous broadening). Within this spectral diffusion regime, the interpretation of the echo decay differs markedly from standard treatments. If the frequency-frequency correlation function initially decays as $1-t^{\beta}$, the echo decay time T_E is proportional to $\tau_m^{\beta/(\beta+2)}$. These results reduce to those of Yan and Mukamel [J. Chem. Phys. **94**, 179 (1991)] for $\beta=1$. Drawing on a viscoelastic model, the theoretical results are compared to viscosity and temperature dependent vibrational echo experiments on myoglobin–CO. A $\tau_m^{1/3}$ dependence is observed, as is predicted for an exponential decay of the frequency–frequency correlation function. © *2000 American Institute of Physics.* [S0021-9606(00)51132-5]

I. INTRODUCTION

Although an isolated spectroscopic transition is a useful ideal, in most real systems, the spectroscopic transitions are perturbed by a variety of interactions, both static and dynamic. Echo spectroscopy is a well-known and general method for discriminating between interactions occurring on different time scales. The two-pulse echo experiment was first introduced as the nuclear magnetic resonance (NMR) spin echo in 1950.[1] Essentially the same pulse sequence was applied to electronic excited states as the photon echo in 1964.[2] Recently, this sequence has been applied on ultrafast time scales to molecular vibrations in condensed matter systems[3] and called the Raman[4–9] or infrared vibrational echo.[10–20] Similar ideas are being used in fifth-order echoes, which have been applied primarily to intermolecular, rather than intramolecular, vibrations.[3,21]

Standard treatments of echo spectroscopy describe two extreme limits.[22–24] Very fast processes, which produce homogeneous dephasing and a motionally narrowed spectroscopic line, and very slow or static processes, which produce an inhomogeneously broadened spectroscopic line. In standard applications, the echo experiment extracts the homogeneous linewidth from a transition dominated by inhomogeneous broadening. However, there is a broad range of modulation times between these limits, where the echo behaves quite differently from these standard treatments. Processes with such intermediate modulation times cause what is often called spectral diffusion. Although the effect of spectral diffusion on two-pulse echoes has been noted before,[25–27] there has been little work exploiting this technique for the study of spectral diffusion.[28] In this paper, we explore the consequence of spectral diffusion for two-pulse echo in more depth, with an aim toward facilitating the interpretation of experimental data. A recent example of two-pulse infrared echoes on the CO vibration of myoglobin is used to illustrate the utility of the resulting ideas. With proper interpretation, the two-pulse echo becomes a powerful tool for measuring the spectral diffusion processes which are common in condensed-phase systems.

Modulation times τ_m are classified with respect to the typical size of the frequency perturbation Δ_m.[29,30] If $\Delta_m\tau_m \ll 1$, the process is motionally narrowed and the dephasing/linewidth is homogeneous. The echo measures a dephasing time T_2 in the sense of the Bloch equations.[24] It does not measure the modulation time directly, although T_2 and τ_m can be related by an appropriate model.

If the modulation time is long enough to prevent motional narrowing, $\Delta_m\tau_m \gg 1$, but fast enough to be experimentally significant, the process is classified as spectral diffusion. Spectral diffusion can be studied using three-pulse stimulated echoes[22–24,27] or the time-dependent versions of hole burning or fluorescence line narrowing.[31–33]

Relatively little attention has been paid to two-pulse echoes in the spectral diffusion range. Older work focused on models appropriate for spin resonance[34–36] or gas-phase collisions.[28] General expressions for the echo signal with arbitrary modulation times were derived by Loring and Mukamel.[37] Yan and Mukamel looked at the case of an exponential spectral diffusion process embedded in a broad inhomogeneous line.[25] They pointed out that in this case, the two-pulse echo decay is cubic on a semilog plot and the characteristic decay time is proportional to the cube-root of the modulation time. We and our coworkers previously looked at the special case of a distribution of modulation times spread over a very broad, continuous range spanning the fast modulation and spectral diffusion ranges.[31,38–40] This case frequently occurs in low temperature glasses. We

a)Telephone: 803-777-1514; Fax: 803-777-9521. Electronic mail: berg@mail.chem.sc.edu
b)Present Address: Los Alamos National Laboratory, Los Alamos, NM 87544.

showed that the two-pulse echo measures a slower time (narrower line) than the stimulated echo, or any other four-time correlation-function experiment. However, we did not examine the effect of changing a single well-defined modulation time across this region.

In the following, we analyze the influence of modulation time on the two-pulse echo observable. In Sec. II, we reexamine a simple, but common model in which the dynamic process decays exponentially and is embedded in a very broad inhomogeneous line.[25,27,29,30] When the modulation is fast, we recover the standard echo result. The echo decay time T_E is equal to a dephasing time T_2 in the sense of the Bloch equations. The process is motionally narrowed, so as τ_m increases, T_E decreases. However, as τ_m continues to increase into the spectral diffusion range, there is a turn over, and subsequent increases in τ_m are directly mirrored in increases of T_E. The echo no longer measures a dephasing time in the Bloch sense, and the interpretation of the echo time as an inverse linewidth breaks down. In the spectral diffusion regime, the echo decay is more directly related to the underlying modulation time, specifically $T_E \propto \tau_m^{\beta/(\beta+2)}$, where β is related to the early time behavior of the modulation. This dependence is often weak, making the echo useful over a very wide range of modulation rates.

Recently a number of detailed vibrational echo studies have been performed on the CO stretching mode of the proteins, myoglobin–CO (Mb–CO)[13–16,41] and hemoglobin–CO.[42] In Sec. III, a $T_E \propto (\eta/T)^{1/3}$ dependence is found experimentally in the myoglobin system.[13–16,41,42] Of particular interest here are studies as a function of solvent viscosity, which is equivalent to changing τ_m. A viscoelastic model[43–45] provides the relationships between τ_m and the solvent viscosity η, and between the magnitude of the frequency fluctuations Δ_m and the temperature T. Two types of data will be considered: Data from temperature-dependent experiments, in which the solvent viscosity changes rapidly with temperature,[16] and isothermal experiments, in which a number of solvents with various viscosities are used.[45] It is found that part of the dephasing is dependent on the solvent viscosity; the remainder persists even at infinite viscosity. The viscosity dependent portion of the protein's structural fluctuations are associated with the dynamics of the protein's surface.[43–45] Using this model, the viscosity dependence of the echo data is found to match the predictions for spectral diffusion driven by an exponentially relaxing environment.

Section IV removes the restrictions on the inhomogeneous width and shape of the correlation function that were present in Sec. II. In the standard echo model based on fast modulation, the presence or absence of inhomogeneous broadening significantly changes the interpretation of the echo decay time.[23,37] In the spectral diffusion range, the echo behavior is unaffected by the presence of an inhomogeneous process in addition to the dynamic one. In fact, the spectral diffusion process does not need to be embedded in a static, inhomogeneous line for the echo to be effective.

Section IV also shows that the exponent relating T_E and τ_m is sensitive to the short-time derivative of the frequency–frequency correlation function. Thus, echo experiments can distinguish between correlation functions with different shapes, e.g., exponential, Gaussian, and stretched exponential.

Section V briefly looks at the shape of the echo decay, which is predicted to be nonexponential in the spectral diffusion range. The shape is also diagnostic of the short-time derivative of the frequency–frequency correlation function.

II. ECHO DECAY TIMES FOR ARBITRARY MODULATION TIMES

We start with a standard stochastic model for echo spectroscopy in which the material is represented as two spectroscopic levels separated by a time-dependent frequency $\omega(t)$.[27,29,30] The deviation of the frequency from its average, $\delta\omega(t) = \omega(t) - \langle \omega(t) \rangle$, is the sum of two stochastic processes

$$\delta\omega(t) = \delta\omega_m(t) + \delta\omega_{\mathrm{sl}}(t). \tag{1}$$

The process causing $\delta\omega_{\mathrm{sl}}(t)$ is very slow or static, has a mean-squared magnitude

$$\Delta_{\mathrm{sl}}^2 = \langle \delta\omega_{\mathrm{sl}}^2 \rangle, \tag{2}$$

and corresponds to inhomogeneous broadening in standard treatments. Our interest is focussed on the process causing $\delta\omega_m(t)$, which is characterized by a mean-squared magnitude

$$\Delta_m^2 = \langle \delta\omega_m^2(0) \rangle, \tag{3}$$

and a frequency–frequency correlation function

$$C_\omega(t) = \frac{1}{\Delta_m^2} \langle \delta\omega_m(t)\, \delta\omega_m(0) \rangle. \tag{4}$$

This process is also has a characteristic decay time τ_m, which can be taken to be the integral decay time

$$\tau_m^i = \int_0^\infty C_\omega(t)\,\mathrm{d}t. \tag{5}$$

(In Sec. IV, a slightly different choice for the characteristic time will be used.) In standard treatments, this correlation function is assumed to decay rapidly, and it creates homogenous broadening. We will allow arbitrary decay times.

Assuming Gaussian statistics and making a cumulant expansion, the decay of the two-pulse echo signal with pulse separation τ has been derived by Mukamel.[27,37] In the limit of delta-function light pulses

$$S_E(\tau) = \int_0^\infty \exp\left\{ -4(\Delta_m \tau_m)^2 \left[C_\varphi\left(\frac{t}{\tau_m}\right) - \frac{1}{2} C_\varphi\left(\frac{t+\tau}{\tau_m}\right) + C_\varphi\left(\frac{\tau}{\tau_m}\right) \right] \right\} \exp[-\Delta_{\mathrm{sl}}^2 (t-\tau)^2]\,\mathrm{d}t, \tag{6}$$

Equation (6) is written in terms of

$$C_\varphi(x) = \int_0^x \int_0^{x'} C_\omega(x'' \tau_m)\,\mathrm{d}x''\,\mathrm{d}x', \tag{7}$$

which is a unitless function of the scaled time, $x = t/\tau_m$.

Using the same definitions, the signal from a free-induction-decay (FID) experiment (the Fourier transform of the absorption line shape) is

$$S_{\mathrm{FID}}(\tau)=\exp\left[-2(\Delta_m\tau_m)^2C_\varphi\left(\frac{\tau}{\tau_m}\right)\right]\exp[-\Delta_{\mathrm{sl}}^2\tau^2]. \quad (8)$$

We also consider a hypothetical FID experiment in which the effects of the nearly static process (inhomogeneous broadening) are completely removed

$$\overline{S}_{\mathrm{FID}}(\tau)=\exp\left[-2(\Delta_m\tau_m)^2C_\varphi\left(\frac{\tau}{\tau_m}\right)\right]. \quad (9)$$

Experimental decay times are defined as the integral of the full decay, i.e., for the echo

$$\frac{T_E}{4}=\frac{1}{S_E(0)}\int_0^\infty S_E(\tau)\mathrm{d}\tau, \quad (10)$$

and for the FID without inhomogeneous broadening

$$\frac{\overline{T}_{\mathrm{FID}}}{2}=\frac{1}{\overline{S}_{\mathrm{FID}}(0)}\int_0^\infty \overline{S}_{\mathrm{FID}}(\tau)\mathrm{d}\tau. \quad (11)$$

If the signals decay exponentially, these expressions give the standard decay times, but this definition of a decay time is also applicable to nonexponential decays. These definitions allow us to postpone discussion of the decay shape until Sec. V.

Initially, we take the limit of very large inhomogeneous broadening, $\Delta_{\mathrm{sl}}\to\infty$. In this case

$$\Delta_mT_E=4(\Delta_m\tau_m)\times\int_0^\infty \exp-4(\Delta_m\tau_m)^2(2C_\varphi(x)-\tfrac{1}{2}C_\varphi(2x))]\mathrm{d}x \quad (12)$$

and

$$\Delta_m\overline{T}_{\mathrm{FID}}=2(\Delta_m\tau_m)\int_0^\infty \exp[-2(\Delta_m\tau_m)^2(C_\varphi(x))]\mathrm{d}x. \quad (13)$$

Regardless of the form or decay rate of the frequency–frequency correlation function, the echo decay time is a only a function of the modulation time, if both times are scaled by the modulation amplitude. In Sec. IV, an example is shown where these relationships transfer to an experimental viscosity and temperature scaling of the echo decay time [see Eq. (23)].

For large and small modulation times, Eqs. (12) and (13) reduce to standard results. In the limit of fast modulation, i.e., $\Delta_m\tau_m\ll 1$, the integrand of Eq. (7) decays very rapidly, so Eqs. (12) and (13) yield

$$\Delta_mT_E=\frac{1}{\Delta_m\tau_m}, \quad (14)$$

$$\Delta_m\overline{T}_{\mathrm{FID}}=\frac{1}{\Delta_m\tau_m}. \quad (15)$$

The echo gives the same result as a hypothetical FID experiment with the inhomogeneous broadening removed. Its decay time is equal to the standard motionally narrowed homogeneous dephasing time $T_E=T_2=1/\Delta_m^2\tau_m$.[29,46]

The case of particular interest here is that of an intermediate modulation time, where τ_m is slow compared to the inverse magnitude of the energy fluctuations, i.e., $\Delta_m\tau_m\gg 1$, but is still fast compared to the very slow or static process responsible for inhomogeneous broadening. In this limit, the integrand in Eq. (12) decays toward zero for small values of x. If the frequency–frequency correlation function is taken to be an exponential

$$C_\omega(t)=\exp\left(\frac{-t}{\tau_m}\right), \quad (16)$$

and only the lowest order terms in $x=t/\tau_m$ are retained, Eq. (12) reduces to

$$\Delta_mT_E=(\tfrac{4}{3})^{2/3}\Gamma(\tfrac{1}{3})(\Delta_m\tau_m)^{1/3}, \quad (17)$$

where $\Gamma(x)$ is the standard gamma function.[47] This result is essentially the same as that derived by Yan and Mukamel from a closely related Brownian oscillator approach.[25] In the extreme limit that $\tau_m\to\infty$, the echo does not decay. This result corresponds to the standard finding that static inhomogeneous broadening does not cause echo decay. However, if the frequency fluctuations are on an intermediate time scale, i.e., they are spectral diffusion, the relatively slow modulations of the frequency do cause the echo to decay. For the exponential correlation function considered here, the echo decay time is proportional to $\tau_m^{1/3}$. However, Sec. IV will show that this result is not general for other correlation functions.

The key point is that the interpretation of the echo decay changes between the fast modulation and spectral diffusion regimes. Unlike the fast modulation case, the echo decay time in the spectral diffusion regime does not correspond to the inverse linewidth of a simple frequency-domain experiment. Nor does it correspond to a dephasing time in the standard sense. Rather the echo decays on a time scale directly determined by the frequency-modulation time τ_m. Furthermore, in the spectral diffusion regime, the echo decay increases with the modulation time, but with a weak power-law dependence. This contrasts with the fast modulation case, where the echo decay time is inversely proportional to the modulation time.

Figure 1 illustrates these ideas with numerical calculations of Eqs. (12) and (13) for arbitrary values of $\Delta_m\tau_m$ and an exponential frequency–frequency correlation function [Eq. (16)]. The scaled echo (solid curve) and modified-FID (dashed curve) decay times are shown on a log plot against the scaled modulation time. In the fast modulation regime, shown on the left side of the plot, the echo experiment is the same as a FID in which the inhomogeneous broadening is eliminated. Both decay times decrease as the modulation time increases. This region corresponds to motionally narrowed, homogeneous line broadening. The echo decay time is the conventionally defined homogeneous dephasing time.

As the modulation slows past $\Delta_m\tau_m\sim 1$, the FID makes a transition from ''homogeneously'' broadened to ''inhomogeneously'' broadened, and the FID-decay time (linewidth) becomes independent of the modulation rate. Because static inhomogeneous broadening (Δ_{sl}) was not included in the FID calculation, the width of the FID line (Fourier transform

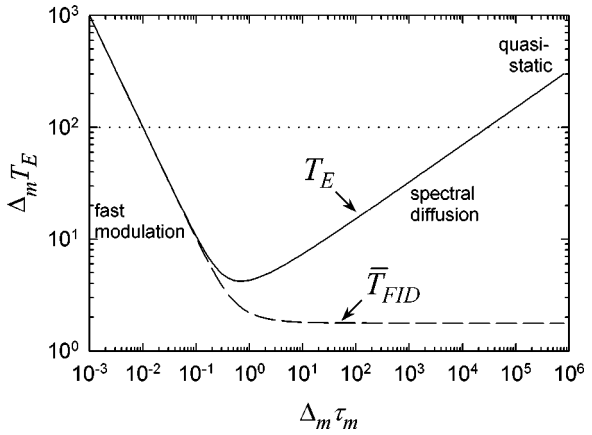

FIG. 1. The scaled echo (solid curve) and modified-FID (dashed curve) decay times calculated for an exponential frequency–frequency correlation function are shown on a log plot against the scaled modulation time τ_m. The standard results are obtained for fast modulation ($\Delta_m \tau_m \ll 1$, motional narrowing regime). As the modulation slows, the spectral diffusion regime ($\Delta_m \tau_m \gg 1$) is entered. The FID makes a transition from ''homogeneously'' broadened to ''inhomogeneously'' broadened, and the FID-decay time (inverse linewidth) becomes independent of the modulation rate. In contrast, the echo decay time is still affected by the modulation. The echo-decay time increases with the modulation time, asymptotically reaching the cube-root dependence of Eq. (17). Other processes set a cutoff on the maximum observable echo decay time (dotted line). The quasi-static approximation is appropriate when the echo decay time exceeds this cutoff.

of the FID decay) reflects Δ_m. In contrast, the echo decay time is still affected by the modulation. The echo decay time increases with the modulation time, asymptotically reaching a cube-root dependence on τ_m.

In any system at equilibrium, there are no truly static processes, only relatively slow ones. Thus it is important to consider what condition allows a process to be treated as quasi-static in an echo experiment. In most systems, additional processes that we have not considered explicitly will also cause dephasing with a decay time T_2'. Even if there are no other pure dephasing processes, the excited-state lifetime T_1 is an additional contribution to the total dephasing. Decays arising from the τ_m-process cannot be observed if they are much longer than the dephasing time resulting from these other processes. This cutoff time is illustrated as a dashed line in Fig. 1. If the modulation time is sufficiently long, the contribution to T_E from spectral diffusion exceeds this cutoff, and the effects of the τ_m-process become unobservable. The quasi-static limit, $\tau_m \to \infty$, is appropriate in this case, and we recover the standard result that a sufficiently slow process is eliminated from the echo decay. However, the distinction between spectral diffusion and the quasi-static regime is not inherent to the modulation process itself; it is determined by competition with other dephasing processes.

Using a unified treatment of the echo across both fast modulation and spectral diffusion regimes, the range of modulation times where the echo can be measured is approximately

$$\frac{1}{T_2' \Delta_m^2} \lesssim \tau_m \lesssim \Delta_m^2 T_2'^3. \tag{18}$$

As an example, if T_1 is the only contribution to the limiting dephasing time T_2', and if we assume a typical vibrational lifetime, then environmental modulation times from $\sim 10^{-13}$ to $\sim 10^{-7}$ s could be detected by vibrational echo experiments. Thus, two-pulse echo experiments have a dynamic range for modulation times much larger than the range of pulse separations. The apparently paradoxical aspects of this result are clarified in Sec. IV.

III. COMPARISON WITH EXPERIMENTS ON PROTEIN DYNAMICS

The properties of the echo derived above are well illustrated by the example of myoglobin–CO. In this system, the solvent modulates the protein, and in turn, the protein modulates the CO. The resulting fluctuation of the CO frequency lies within the spectral diffusion regime. Thus the echo decay times are directly related to the rate of solvent-induced modulations of the protein structure. Another publication will thoroughly discuss the experimental results and their meaning in terms of protein structural fluctuations.[45] Here, we present a limited amount of data and only sufficient background so that the experimental results can be compared to the predictions of the theory presented above, in particular to Eq. (17).

Recently, the ultrafast infrared vibrational echo technique has been applied to the study of the protein dynamics of myoglobin–CO (Mb–CO)[13–16,41] and hemoglobin–CO.[42] The vibrational echo measurements of the pure dephasing of the CO stretching mode are sensitive to the complex protein dynamics communicated to the CO ligand bound at the active site of the protein.[13–16,41] Unlike other ultrafast techniques,[48,49] which involve electronic excitation of chromophores, the vibrational echo experiments directly examine fluctuations of protein structure on the ground-state potential surface.

The experimental method and procedures have been discussed in detail previously.[13–16,41] Infrared (IR) pulses of ~ 1 ps duration and ~ 15 cm^{-1} bandwidth are tuned to the A_1 CO stretching mode of Mb–CO. Two pulses are crossed in the sample at a small angle. The echo signal is detected at the phase matching angle as a function of τ, the delay time between the two excitation pulses. The temperature was varied using a constant-flow cryostat. At each temperature, a vibrational-echo decay and a pump–probe decay were recorded. Within experimental error, both decays could be fit to exponentials. The echo decay gives T_E, and the pump–probe decay gives the $\nu = 1$ lifetime T_1. The pure dephasing time T_E^* is determined from

$$\frac{1}{T_E} = \frac{1}{T_E^*} + \frac{1}{2T_1}. \tag{19}$$

In the derivations given above, T_1 was not included, so T_E^* corresponds to the echo times calculated above.

An IR vibrational-echo study was performed on Mb–CO in a variety of solvents at room temperature (295 K).[45] The solvents were chosen to have a wide range of viscosities. The viscosity of each solvent with protein was measured. The pure dephasing data display a significant dependence on the solvent viscosity. The mechanism of coupling of protein

structural fluctuations to the CO vibrational transition frequency has been discussed in detail previously.[15] Here we are interested in the role that the protein's surface motions, which are sensitive to the solvent viscosity, have on the CO pure dephasing.

In addition to the isothermal experiments, temperature dependent IR vibrational echo experiments on Mb–CO in the solvents trehalose and a 50:50 (v:v) ethylene glycol:water (pH 7 0.1 M sodium phosphate buffer) mixture (hereafter referred to as EgOH) were performed.[16] The temperature dependent pure dephasing in the two solvents are identical below ~150 K. However, the dynamics are dramatically different above this temperature. In the experiments with Mb–CO in trehalose, the solvent is a glass at all temperatures studied (10–310 K). The data arise from the protein dynamics with fixed, essentially infinite, viscosity, and therefore, there is no significant change in the protein surface dynamics with temperature. The surface topology is fixed. The EgOH sample displays a much steeper temperature dependence than the trehalose sample does above the EgOH glass-transition temperature at ~130 K. The change in the pure dephasing with temperature is caused by a combined viscosity and temperature dependence. Between 130 and 295 K, the EgOH viscosity changes by more than ten orders of magnitude, but the pure dephasing (attributed to the viscosity change, see below) only changes somewhat more than one order of magnitude. This initially surprising disparity is attributed to the weak dependence of T_E on τ_m in the spectral diffusion regime, as discussed in Sec. II.

We wish to determine the influence of changing the viscosity on the echo decay. At room temperature, the trehalose sample displays significant pure dephasing despite the fact that the viscosity is essentially infinite. The pure dephasing rate in trehalose represents the infinite viscosity point. The pure dephasing in this sample is only due to temperature induced structural fluctuations of the protein that do not require participation of solvent motion to any significant extent. To obtain the room-temperature viscosity dependence, the room-temperature infinite-viscosity pure dephasing rate (the rate in trehalose) is subtracted from the pure dephasing rates measured at finite viscosities

$$\frac{1}{T_E^r(\eta)} = \frac{1}{T_E(\eta,T)} - \frac{1}{T_E(\eta=\infty,T)}, \tag{20}$$

where T_E^r is the reduced pure dephasing time. The contribution from T_1 was removed before hand by using Eq. (19). In the nomenclature of Sec. II, T_E^r is the dephasing time from the primary spectral diffusion process, and $T_E(\eta=\infty)$ corresponds to the external dephasing time T_2'. Equation (20) implies that the temperature dependence at infinite viscosity and the viscosity dependence are additive. The additivity will be discussed below and shown to be a reasonable model.

The viscosity dependence of the pure dephasing data taken in EgOH as a function of temperature was determined in the same manner. In the EgOH experiments, the viscosity varied by changing temperature rather than by changing the solvent. To obtain the influence on the pure dephasing that is associated with a change in viscosity, at each temperature, the contribution to the pure dephasing measured in trehalose (infinite viscosity) was removed from the EgOH data using Eq. (20).

To compare the experimental results of the temperature dependent study in EgOH with the isothermal viscosity study, the temperature dependent viscosity of the EgOH sample, including the protein, was measured between 210 K and room temperature.[45] The viscosities at lower temperatures were obtained using a Vogel–Tammann–Fulcher (VTF) equation to model the viscosity.[50–52] A VTF curve was fit to the measured points along with the assumption that the viscosity is 10^{13} cP at T_g of the solvent alone (136 K). A viscosity of 10^{13} cP is frequently used to define the laboratory glass transition temperature. However, a single VTF curve cannot accurately emulate the viscosity over such as large temperature range. Furthermore, T_g of the solvent plus protein will differ somewhat from the solvent alone. Therefore, the viscosities at the lowest temperatures are approximate.

As has been discussed briefly previously[16] and will be discussed in detail subsequently,[45] the experimental data described above suggest the following model for the role of the solvent viscosity. When the protein is in a solid, glassy solvent, the surface topology of the protein is essentially fixed. The protein can still undergo structural fluctuations, but only those fluctuations that do not change the protein's surface topology are permitted. The surface of the protein can only change in so far as the glass in which it is embedded is compressible. Because the compressibility of a glass is very small, surface motions of the protein are severely restricted. Thus, the protein is limited to internal motions. The temperature dependence of such motions, as sensed by CO bound at the active site of Mb, is reflected in the temperature-dependent pure dephasing measured in trehalose. In EgOH below its T_g, the behavior of Mb–CO is identical to its behavior in trehalose.[16]

Above T_g, the EgOH surrounding the protein is a liquid. Thus the protein is no longer constrained only to have motions that maintain the protein's surface topology. The additional protein motions are modeled by the Δ_m and τ_m of Sec. II. The response of the liquid is time dependent and is characterized by its time-dependent viscoelastic properties.[53] Just above T_g, the liquid is extremely viscous, and its response to protein structural fluctuations that would change the protein surface is extremely slow. The modulation time τ_m is very long. Other processes, i.e., T_1 and the internal structural fluctuations that are observed in trehalose, dominate the dephasing. This competition puts the solvent-induced process in the quasi-static limit, and its contribution to the echo is negligible. As the temperature is increased above T_g, the liquid's ability to respond to protein structural fluctuations increases, and τ_m becomes shorter. At some temperature, τ_m becomes short enough that the contributions to the pure dephasing caused by the protein's surface fluctuations become comparable to the other dephasing processes. A new contribution to the Mb–CO homogeneous pure dephasing comes into play as the solvent-induced modulations enter the spectral diffusion regime. Protein motions that do not involve the protein's surface still occur, but as the viscosity of the solvent

drops, structural fluctuations that involve surface dynamics become an increasingly important contribution to the pure dephasing. It is not the motions of the surface per se that cause pure dephasing, but rather, motions of the surface permit structural fluctuations of the protein that are not possible in a glassy solvent that locks in the surface topology. Such motions involve internal components of the protein as well as the surface.

Recently, a viscoelastic continuum theory was developed to describe electronic-state solvation dynamics as well as vibrational absorption linewidths.[43,44,54,55] The theory has had considerable success in reproducing important features of these experiments. We have adapted the viscoelastic theory to analyze the vibrational echo data on Mb–CO.[45] The full development of the theory in application to the Mb–CO experiments and a complete discussion of the data analysis will be presented elsewhere.[45] Here, we only need two features of the viscoelastic theory,[43,44]

$$\Delta_m \propto T^{1/2}, \tag{21}$$

where T is the temperature in Kelvin, and

$$\tau_m \propto \eta, \tag{22}$$

where η is the solvent viscosity. If the solvent-induced component of the frequency fluctuation are in the spectral diffusion regime, Eq. (17) predicts that

$$T^{1/2}T_E^r = A(T^{1/2}\eta)^{1/3}, \tag{23}$$

where A is a constant. [Equation (23) can be rewritten in the simpler form.

$$T_E^r = A\left(\frac{\eta}{T}\right)^{1/3}. \tag{24}$$

However, Eqs. (12), (21), and (22) show that $T^{1/2}T_E^r$ is a function of $T^{1/2}\eta$ even outside the spectral diffusion range and regardless of the form of the frequency–frequency correlation function. Thus, Eq. (23) is a more robust way to analyze the data.]

Figure 2 displays the Mb–CO solvent induced echo decay data on a log plot. Two types of data are displayed. The squares are the isothermal data measured at 295 K in solvents of various viscosities with the infinite viscosity contribution to the pure dephasing (Mb–CO in trehalose) removed [Eq. (20)]. The circles are the temperature-dependent data measured in EgOH with the infinite viscosity contribution to the pure dephasing (Mb–CO in trehalose) removed at each temperature [Eq. (20)]. (The temperatures are scaled by 295 K, so the factor of $T^{1/2}$ is 1 for the isothermal data.) Note that the two types of data are intermixed. It does not matter whether the data is taken at constant temperature in several solvents with only the viscosity changing, or the if the data is taken in EgOH as a function of temperature, which results in a viscosity change. This supports the additivity of the two terms in Eq. (20).

The important feature of Fig. 2 is the solid line through the data. The line is a graph of Eq. (23); only the amplitude factor A was adjusted. Within experimental error, the agreement between the prediction and experiment is very good.

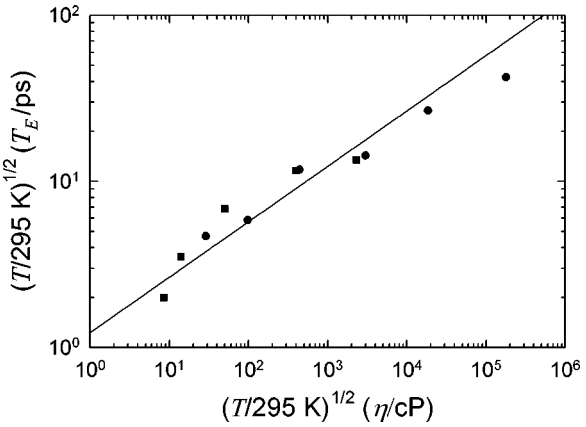

FIG. 2. Mb–CO solvent induced pure dephasing times versus solvent viscosity on a log plot. The isothermal (295 K) data (■) were taken in solvents of various viscosities. For data measured in EgOH (●), the temperature was used to change the viscosity. The two types of data are intermixed. The temperatures are scaled by 295 K, so the factor of $T^{1/2}$ is 1 for the isothermal data. The solid line through the data is a graph of Eq. (23); only the amplitude factor A was adjusted. Within experimental error, the agreement between the prediction and experiment is very good. The predicted cube-root dependence on τ_m is observed.

These data illustrate the fundamental features of spectral diffusion. If the system were in the motional narrowing regime, i.e., fast modulation with $\Delta_m \tau_m \ll 1$, the dephasing time would increase as the viscosity decreased. Here we see that as the viscosity and resulting modulation time decrease, the homogeneous dephasing time decreases, as is characteristic of spectral diffusion. Furthermore, it decreases with the cube-root form of Eq. (23). At low temperature, where τ_m becomes sufficiently long, other processes, e.g., T_E^r and T_1, dominate the echo decay. The slow frequency evolution is then part of the inhomogeneous broadening, and it does not contribute to the echo decay. For the protein, this condition occurs at temperatures below ~190 K and viscosities above $\sim 2\times 10^5$ cP.

IV. ARBITRARY CORRELATION FUNCTIONS IN INTERMEDIATE MODULATION

Section II confined itself to the case where the spectral diffusion is embedded within a broad inhomogeneous line, and the frequency–frequency correlation function decays exponentially. Both restrictions can be lifted, if we confine our results to the spectral diffusion range.

In the spectral diffusion regime, we represent the frequency correlation function to low order by

$$C_\omega(t) = 1 - \left(\frac{t}{\tau_m}\right)^\beta + \cdots. \tag{25}$$

The value of β is determined by the shape of the correlation function at early times. An exponential correlation function [Eq. (5)] corresponds to $\beta=1$. Using $\beta=2$ includes functions like the Gaussian, $\mathrm{sech}^2(t)$,[56] and the ''ansatz'' popularized by Skinner.[57,58] Stretched exponential correlation functions, $\exp[-(t/\tau_m)^\beta]$, are covered by values of $0<\beta<1$.

For nonexponential decays, there is not a unique choice of a time constant to characterize the decay. In the fast

modulation regime, it is known that the FID and echo decay times [Eqs. (14) and (15)] are not sensitive to the shape of the correlation function, so long as the exponential time constant τ_m is replaced by the integral decay time τ_m^i defined in Eq. (5). In the spectral diffusion regime, the echo decay depends most directly on the initial decay time $\mathring{\tau}_m$. This time is defined by the short-time expansion in Eq. (25). For an exponential, it is equal to both the time constant and integral decay time, $\tau_m^i=\tau_m=\mathring{\tau}_m$. For other decay shapes, these times differ. For example, with a Gaussian decay, $\exp[-(t^2/2\tau_m^2)]$, the times are related by $2(2\pi)^{-1/2}\tau_m^i=\tau_m=2^{1/2}\mathring{\tau}_m$. For a stretched exponential, the relationship is $\beta\tau_m^i/\Gamma(\beta^{-1})=\tau_m=\mathring{\tau}_m$. Unlike the fast modulation limit, the shape of the correlation function, in the form of the exponent β, also plays a role.

Putting the expansion Eq. (25) in Eqs. (6) and (10) yields

$$\Delta_m T_E = B_\beta(\Delta_m\mathring{\tau}_m)^{\beta/(\beta+2)}\frac{\beta+2}{2} \times\int_0^\infty e^{-x^3}\Phi\left(\frac{(\beta+2)}{4}B_\beta\left(\frac{\Delta}{\Delta_m}\right)\times(\Delta_m\mathring{\tau}_m)^{2/(\beta+2)}x\right)dx, \tag{26}$$

where the full linewidth is given by

$$\Delta^2=\Delta_m^2+\Delta_{sl}^2, \tag{27}$$

the standard error function $\Phi(x)$ is used,[47] and

$$B_\beta=\frac{1}{2}\left(\frac{8}{\beta+2}\right)^{(\beta+1)/(\beta+2)}\left(\frac{\beta+1}{2^\beta-1}\right)^{1/(\beta+2)} \tag{28}$$

is a constant determined by β.

In Sec. II, the limit of an infinitely broad inhomogeneous linewidth, $\Delta/\Delta_m\gg1$, was invoked. In Eq. (26), this limit allows the error function to be replaced with unity over the important regions of the integrand. In the case where $\beta=1$, this limit leads to Eq. (17). However, Eq. (26) shows that essentially the same result

$$\Delta_m T_E=\frac{1}{2}B_\beta\Gamma\left(\frac{1}{\beta+2}\right)(\Delta_m\mathring{\tau}_m)^{\beta/(\beta+2)}, \tag{29}$$

occurs in the spectral diffusion region, $\Delta_m\tau_m\gg1$, regardless of the amount of inhomogeneous broadening. Thus, in the spectral diffusion regime, the presence of an additional inhomogeneous broadening is irrelevant to the formation and behavior of the echo.

Removing the need for an extra inhomogeneous process has practical significance. In the protein system, $\Delta=15\,\mathrm{cm}^{-1}$, corresponding to an inverse time of 2 ps. At the lowest viscosities, solvent modulation times τ_m are predicted to be on the order of 10 ps or even less. Under these conditions, it is hard to understand how both the spectral diffusion and broad inhomogeneity limits, $\tau_m\gg\Delta_m^{-1}\gg\Delta^{-1}$, can be satisfied. With the realization that only one limit is essential, $\tau_m\gg\Delta_m^{-1}$, the experimental results are more easily reconciled with theory.

This behavior is linked to the fact that the echo time is only sensitive to the properties of the frequency correlation function at early times. Equation (29) only includes $\mathring{\tau}_m$ and β, which are early time properties of $C_\omega(t)$. In the spectral diffusion regime, the echo signal decays much more rapidly than the frequency correlation function, so the echo experiment only samples the initial part of the correlation function. As a result, the echo is insensitive to whether the correlation function decays to zero on a single time scale (i.e., spectral diffusion with additional inhomogeneous broadening) or reaches a constant at some later time (i.e., spectral diffusion with additional inhomogeneous broadening).

The fact that the echo is only sensitive to the initial modulation time also explains the wide range of modulation times that can be monitored with the two-pulse echo. The echo yields the initial slope of the frequency–frequency correlation function, which in principle can be determined in an arbitrarily short time. As is expected, the two-pulse echo does not give information on the frequency correlation near or beyond the $1/e$ time of the correlation function, which are at times much longer than the echo pulse separation.

This early time sensitivity complements another method of measuring spectral diffusion, the three-pulse stimulated echo.[23,24] In that experiment, the first two pulses are separated by a time τ_1, which is fixed at a value larger than the inverse linewidth. The separation of the second and third pulses τ_2 is scanned. The decay of the signal with τ_2 gives a direct measure of $C_\omega(t)$ and thus of the spectral diffusion time. However, the stimulated echo is most effective for times near the $1/e$ time of $C_\omega(t)$ and longer. The early part of the $C_\omega(t)$ is difficult to observe because of the small amplitude of the changes in $C_\omega(t)$ and the need to keep τ_1 at a finite value.

Equation (29) also shows that the variation of the echo decay time with the modulation time is a measure of β, the initial shape of $C_\omega(t)$. In Sec. III, the modulation time was proportional to the viscosity of the system. Thus, Fig. 2 demonstrates that the correlation function in a protein has a linear initial decay. The data are consistent with a simple exponential $C_\omega(t)$, but are not compatible with a stretched exponential or with a power law, which is predicted for β-relaxation in mode-coupling theories.[59]

By related physical reasoning, any component of $C_\omega(t)$ much faster than the echo decay time can be excluded from the expansion in Eq. (25). This expansion only needs to be valid over the time range where the echo is measurable, i.e., from approximately the excitation pulse width out to a few decay times. For example, all time correlation functions must be quadratic at sufficiently short times. However, this limit often only applies to a very short, inertial component confined to ~100 fs or less. With the picosecond pulses used in Sec. II, any inertial dynamics need not be included in Eq. (25), because they will have decayed before the earliest measurable time. Any effect from inertial dynamics can be included as a separate, homogeneous dephasing process.

V. ECHO DECAY SHAPE

It is important to note that even for an exponential decay of $C_\omega(t)$, the echo decay is not necessarily exponential. For an exponential $C_\omega(t)$ [Eq. (16)], the echo decay shape is

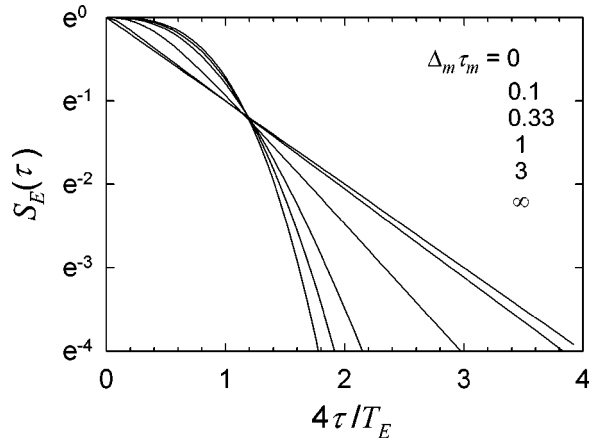

FIG. 3. The shape of the echo decay from Eq. (30) as a function of $\Delta_m\tau_m$ (0, 0.1, 0.33, 1, 3, ∞; top to bottom on the right). In the fast modulation limit ($\Delta_m\tau_m\rightarrow 0$), the decay is exponential, i.e., linear on this semilog plot. In the spectral diffusion range ($\Delta_m\tau_m\rightarrow\infty$), the decay is $\exp[-(t/\tau_m)^3]$, i.e., cubic on this plot. The feasibility of experimentally measuring this characteristic decay shape depends on the signal-to-noise level, the amount of pulse-width broadening and the presence of competing dephasing processes.

$$S_E(\tau)=\exp\left\{-4(\Delta_m\tau_m)^2\left[2\exp\left(\frac{-\tau}{\tau_m}\right)-\frac{1}{2}\exp\left(\frac{-2\tau}{\tau_m}\right)+\frac{\tau}{\tau_m}-\frac{3}{2}\right]\right\}. \tag{30}$$

In a real experiment, this curve is only observed in the region $\tau\sim T_E$. In the fast modulation limit, the echo decays more slowly than τ_m, so the terms in $\exp(-\tau/\tau_m)$ can be dropped in Eq. (30). In this limit, the echo decay is exponential over the experimental time region and has a decay time $T_E/4$. However, in the spectral diffusion range, the echo decay is much faster than τ_m. The terms in $\exp(-\tau/\tau_m)$ can be expanded to lowest order, giving

$$S_E(\tau)=\exp\left[-\left(\frac{4\Gamma(4/3)\tau}{T_E}\right)^3\right]. \tag{31}$$

A plot of $\ln S_E(\tau)$ will be cubic, not linear. This result was originally derived by Yan and Mukamel.[25]

Figure 3 shows Eq. (30) for various values of $\Delta_m\tau_m$. As the modulation time changes from the fast modulation to the spectral diffusion regime, the echo decay makes a definite change in shape.

For a general frequency–frequency correlation function in the spectral diffusion limit, and taking a broad inhomogeneous line, the echo decay shape is

$$S(\tau)=\exp\left[-\frac{8(\Delta_m\tau_m)^2}{(\beta+1)(\beta+2)}\left(\frac{\tau}{\tau_m}\right)^{2+\beta}\right]. \tag{32}$$

On a semilog plot, the echo decays as the $2+\beta$ power of the delay time. Thus the echo decay shape can also be diagnostic for the form of the frequency–frequency correlation function.

In some systems, the change in echo decay shape may be very diagnostic of the type of modulation. However, it should be recognized that the decay shape is a function of both the modulation regime (Fig. 3) and with the form of the correlation function [Eq. (32)].

In other experiments, including those described in Sec. III, other factors obscure the decay shape. There are additional processes, specifically the lifetime T_1 and the infinite viscosity pure dephasing process, that give rise to exponential decays that are convolved with Eq. (30). Convolution with the laser pulse shape and pulse-overlap artifacts further complicate the echo shape. Model calculations matching the conditions in Sec. III indicate that the difference between fast and intermediate modulation shapes is difficult to discern in the experiments discussed in Sec. III. In systems like these, the variation of the echo decay time with viscosity [Eq. (23)] is an important alternative approach to detecting and analyzing spectral diffusion.

VI. CONCLUDING REMARKS

To summarize the nature of the spectral diffusion regime, we compare intermediate modulation and fast modulation in the two limits of large inhomogeneous broadening ($\Delta_{sl}\gg\Delta_m$) and no inhomogeneous broadening ($\Delta_{sl}=0$). First consider the case of large inhomogeneous broadening and fast modulation. The echo experiment eliminates the inhomogeneous broadening and reveals the homogeneously broadened line. The echo decay time is $T_E=T_2=1/\Delta_m^2\tau_m$. For the same system, an absorption spectrum measures a linewidth dominated by Δ_{sl}. Defining an echo linewidth as $1/\pi T_E$, the echo is identical to a hypothetical linewidth experiment where the inhomogeneous broadening is eliminated.

In the spectral diffusion limit with large inhomogeneous broadening, the echo decay time T_E is again determined by Δ_m and τ_m [Eq. (29)], but the functional dependence is different from the case of fast modulation. The echo linewidth can still be defined as the inverse of the echo decay time, $\Gamma_E=(\pi T_E)^{-1}$, and it will be substantially narrower than absorption linewidth. However, there is no frequency domain experiment that readily corresponds to this linewidth. It is easier to interpret the echo decay directly in terms of modulation times.

For zero inhomogeneous broadening and fast modulation, the echo decay time becomes[37] $T_E=2T_2$ and is directly related to the absorption spectrum full width at half maximum (FWHM), which is equal to $1/\pi T_2$. In the spectral diffusion case, the absorption spectrum measures the full spread of frequencies Δ_m and provides no information on τ_m. However, the echo decay time is still determined by both Δ_m and τ_m. Even in the absence of distinct inhomogeneous broadening, the echo decay gives information on the rate of spectral diffusion. The only limitation is that, if τ_m becomes sufficiently slow, other processes, such as T_1, will dominate the echo decay, and Δ_m will take on the role of a quasi-static inhomogeneous broadening, even in an echo experiment.

The well-known phenomenon of motional narrowing and the spectral diffusion results we have presented here apply to what Kubo has called ''Gaussian'' modulation.[30] In

this case, the chromophore frequency is continuously modulated. It applies at higher temperatures, where thermal excitations of the solvent (e.g., phonons) are heavily populated, so the chromophore is being perturbed almost continually. Echoes, either optical or vibrational, are also frequently used on low temperature systems, such as chromophores in crystals[60] or glasses.[32] In these systems, thermal excitations are relatively rare, so the time between interactions with the chromophore (e.g., phonon scattering, population of a low lying vibration) is large compared to the duration of the interaction. These systems correspond to Kubo's ''Poisson'' modulation.[30] Each interaction is uncorrelated with the others and contributes an independent loss of phase memory. These contributions simply accumulate with time. Motional narrowing and the spectral diffusion phenomena presented here do not apply to these systems.

In this paper, we have discussed a number of features of the two-pulse echo in the spectral diffusion limit, with the aim of more effectively interpreting experimental data. The most important results are: (1) The scaling of the echo decay time with viscosity can be used to distinguish between fast modulation, spectral diffusion, and quasi-static dynamics. (2) The exponent of the viscosity dependence determines the short-time behavior of the frequency–frequency correlation function. In this regard, the two-pulse echo complements other echo techniques, which are more effective at later times. (3) The range of modulation rates measurable by the two-pulse echo can be very large, limited only by the intervention of additional dephasing processes. (4) Processes which modulate a transition frequency can only be treated as quasi-static, if the level of these additional dephasing processes is known. (5) In the spectral diffusion regime, inhomogeneous broadening is not required for the two-pulse echo to be effective.

These ideas were illustrated with ultrafast vibrational echo experiments on the CO stretching mode of myoglobin–CO. The dependence of the vibrational echo decay time on the viscosity of the solvent surrounding the protein shows that as the solvent viscosity decreased, the echo decay time decreased. Using a viscoelastic model,[43,44] the change in viscosity is related to the change in τ_m. The $\tau_m^{1/3}$ dependence predicted for exponentially relaxing dynamics was observed.

The results presented above will enhance the usefulness of echo spectroscopy for the study of complex systems such as proteins or solute molecules in liquid solvents. They show that an echo decay need not reflect a motionally narrowed homogeneous line shape. In the intermediate modulation regime, the echo decay reflects the rate of spectral diffusion, i.e., the slow evolution of the transition energy. The echo decay time as a function of system properties, such as temperature or viscosity, can be used as a direct probe of the underlying system dynamics.

ACKNOWLEDGMENTS

We thank Dr. Jianwen Jiang for assistance with the numerical calculations. This material is based upon work supported by the National Science Foundation under Grant No. CHE-9809719 to MAB and Grant No. DMR-008942 to MDF and by the National Institutes of Health under Grant No. 1RO1-GM61137 to MDF.

[1] E. L. Hahn, Phys. Rev. **80**, 580 (1950).
[2] I. D. Abella, N. A. Kurnit, and S. R. Hartmann, Phys. Rev. Lett. **14**, 391 (1966).
[3] M. D. Fayer, *Ultrafast Infrared and Raman Spectroscopy* (Marcel Dekker, New York, NY, in press).
[4] D. Vanden Bout, L. J. Muller, and M. Berg, Phys. Rev. Lett. **67**, 3700 (1991).
[5] L. J. Muller, D. A. Vanden Bout, and M. Berg, J. Chem. Phys. **99**, 810 (1993).
[6] D. Vanden Bout, J. E. Freitas, and M. Berg, Chem. Phys. Lett. **229**, 87 (1994).
[7] D. A. Vanden Bout and M. Berg, J. Raman Spectrosc. **26**, 503 (1995).
[8] M. Berg and D. A. Vanden Bout, Acc. Chem. Res. **30**, 65 (1997).
[9] M. A. Berg, in *Ultrafast Infrared and Raman Spectroscopy*, edited by M. D. Fayer (Marcel Dekker, New York, NY, in press).
[10] D. Zimdars, A. Tokmakoff, S. Chen, S. R. Greenfield, and M. D. Fayer, Phys. Rev. Lett. **70**, 2718 (1993).
[11] A. Tokmakoff and M. D. Fayer, J. Chem. Phys. **103**, 2810 (1995).
[12] A. Tokmakoff, A. S. Kwok, R. S. Urdahl, R. S. Francis, and M. D. Fayer, Chem. Phys. Lett. **234**, 289 (1995).
[13] C. W. Rella, K. D. Rector, A. S. Kwok, J. R. Hill, H. A. Schwettman, D. D. Dlott, and M. D. Fayer, J. Phys. Chem. **100**, 15620 (1996).
[14] K. D. Rector, C. W. Rella, A. S. Kwok, J. R. Hill, S. G. Sligar, E. Y. P. Chien, D. D. Dlott, and M. D. Fayer, J. Phys. Chem. B **101**, 1468 (1997).
[15] K. D. Rector, J. R. Engholm, J. R. Hill, D. J. Myers, R. Hu, S. G. Boxer, D. D. Dlott, and M. D. Fayer, J. Phys. Chem. B **102**, 331 (1998).
[16] K. D. Rector, J. R. Engholm, C. W. Rella, J. R. Hill, D. D. Dlott, and M. D. Fayer, J. Phys. Chem. A **103**, 2381 (1999).
[17] P. Hamm, M. Lim, W. F. DeGrado, and R. M. Hochstrasser, J. Phys. Chem. A **103**, 10049 (1999).
[18] P. Hamm, M. Lim, M. Asplund, and R. M. Hochstrasser, Chem. Phys. Lett. **301**, 167 (1999).
[19] M. H. Lim, P. Hamm, and R. M. Hochstrasser, Proc. Natl. Acad. Sci. USA **95**, 15315 (1998).
[20] P. Hamm, M. Lim, and R. M. Hochstrasser, Phys. Rev. Lett. **81**, 5326 (1998).
[21] S. Mukamel, A. Piryatinski, and V. Chernyak, Acc. Chem. Res. **32**, 145 (1999).
[22] T. C. Farrar and D. E. Becker, *Pulse and Fourier Transform NMR* (Academic, New York, 1971).
[23] M. D. Levenson, *Introduction to Nonlinear Laser Spectroscopy* (Academic, San Jose, 1982).
[24] C. P. Slichter, *Principles of Magnetic Resonance* (Springer-Verlag, Berlin, 1989).
[25] Y. J. Yan and S. Mukamel, J. Chem. Phys. **94**, 179 (1991).
[26] W. B. Bosma, Y. J. Yan, and S. Mukamel, Phys. Rev. A **42**, 6920 (1990).
[27] S. Mukamel, *Principles of Nonlinear Optical Spectroscopy* (Oxford University Press, New York, 1995).
[28] J. Schmidt, P. R. Berman, and R. G. Brewer, Phys. Rev. Lett. **31**, 1103 (1973).
[29] P. W. Anderson, J. Phys. Soc. Jpn. **9**, 316 (1954).
[30] R. Kubo, in *Fluctuation, Relaxation and Resonance in Magnetic Systems*, edited by D. Ter Haar (Oliver and Boyd, London, 1961).
[31] M. Berg, C. A. Walsh, L. R. Narasimhan, K. A. Littau, and M. D. Fayer, J. Chem. Phys. **88**, 1564 (1988).
[32] L. R. Narasimhan, K. A. Littau, D. W. Pack, Y. S. Bai, A. Elschner, and M. D. Fayer, Chem. Rev. **90**, 439 (1990).
[33] J. Ma, J. T. Fourkas, D. A. Vanden Bout, and M. Berg, in *Supercooled Liquids: Advances and Novel Applications*, Vol. 676, edited by J. T. Fourkas, D. Kivelson, U. Mohanty, and K. A. Nelson (American Chemical Society, Washington, DC, 1997), p. 199.
[34] J. R. Klauder and P. W. Anderson, Phys. Rev. **125**, 912 (1962).
[35] P. Hu and S. R. Hartmann, Phys. Rev. B **9**, 1 (1974).
[36] P. Hu and L. R. Walker, Phys. Rev. B **18**, 1300 (1978).
[37] R. F. Loring and S. Mukamel, Chem. Phys. Lett. **114**, 426 (1985).
[38] Y. S. Bai and M. D. Fayer, Phys. Rev. B **39**, 11066 (1989).
[39] L. R. Narasimhan, Y. S. Bai, M. A. Dugan, and M. D. Fayer, Chem. Phys. Lett. **176**, 335 (1991).

[40] K. A. Littau, M. A. Dugan, S. Chen, and M. D. Fayer, J. Chem. Phys. **96**, 3484 (1992).
[41] C. W. Rella, A. Kwok, K. D. Rector, J. R. Hill, H. A. Schwettmann, D. D. Dlott, and M. D. Fayer, Phys. Rev. Lett. **77**, 1648 (1996).
[42] K. D. Rector, D. E. Thompson, K. Merchant, and M. D. Fayer, Chem. Phys. Lett. **316**, 122 (2000).
[43] M. A. Berg and H. W. Hubble, Chem. Phys. **233**, 257 (1998).
[44] M. Berg, J. Phys. Chem. **102**, 17 (1998).
[45] K. D. Rector, M. A. Berg, and M. D. Fayer (in preparation).
[46] R. Kubo, in *Fluctuation, Relaxation, and Resonance in Magnetic Systems*, edited by D. T. Haar (Oliver and Boyd, London, 1962).
[47] I. S. Gradshteyn and I. M. Ryzhik, *Table of Integrals, Series and Products*, 4th ed. (Academic, New York, 1980).
[48] D. T. Leeson, D. A. Wiersma, K. Fritsch, and J. Friedrich, J. Phys. Chem. B **101**, 6331 (1997).
[49] D. T. Leeson and D. A. Wiersma, Phys. Rev. Lett. **74**, 2138 (1995).
[50] C. A. Angell and D. L. Smith, J. Phys. Chem. **86**, 3845 (1982).
[51] C. A. Angell, J. Phys. Chem. Solids **49**, 863 (1988).
[52] G. H. Fredrickson, Annu. Rev. Phys. Chem. **39**, 149 (1988).
[53] N. W. Tschoegl, *The Phenomenological Theory of Linear Viscoelastic Behavior, An Introduction* (Springer-Verlag, Berlin, 1989).
[54] M. Berg, Chem. Phys. Lett. **228**, 317 (1994).
[55] M. A. Berg, J. Chem. Phys. **110**, 8577 (1999).
[56] D. W. Oxtoby, J. Chem. Phys. **74**, 1503 (1981).
[57] D. C. Douglass, J. Chem. Phys. **35**, 81 (1961).
[58] S. A. Egorov and J. L. Skinner, J. Chem. Phys. **105**, 7047 (1996).
[59] W. Götze and L. Sjögren, Transp. Theory Stat. Phys. **24**, 801 (1995).
[60] J. S. Meth, C. D. Marshall, V. J. Newell, and M. D. Fayer, J. Chem. Phys. **92**, 3323 (1990).